Int. J. Mech. Sci. Vol. 35, No. 12, pp. 1035–1052, 1993
Printed in Great Britain.

0020–7403/93 $6.00 + .00

PLASTIC DEFORMATION MECHANISMS IN AXIALLY COMPRESSED METAL TUBES USED AS IMPACT ENERGY ABSORBERS

S. R. REID
Department of Mechanical Engineering, UMIST, P.O. Box 88, Sackville Street, Manchester M60 1QD, U.K.

Abstract—The characteristics of a number of metal components proposed as impact energy absorbers are reviewed, attention being focussed on to modes of deformation which stem from the axial compression of metal tubes. Progressive buckling, inversion and splitting are discussed and areas for future work identified. The buckling of thin-walled square section tubes filled with polyurethane foam is also described. Reference is also made to recent work on cellular materials which highlights the influence of inertia in axially compressed tubes and tubular arrays.

1. INTRODUCTION

The design of crashworthy structures, i.e. structures capable of withstanding and mitigating the effect of impact, requires both a knowledge of structural dynamics and an understanding of the properties and deformation mechanisms of the materials and components used. References [1–4] provide substantial background information on the subject. Most of the work concerned with impact energy absorption has focussed on the behaviour of metal structures and components for which the main energy-dissipating mechanisms are plastic deformation and fracture or tearing. Work on metallic devices continues and some recent results are reviewed in this paper, there being several fundamental problems that still remain unresolved, but there is also a growing interest in components made from non-metals. Fibre-reinforced plastics of various sorts have also been examined for their use in impact energy absorbing structures and reference can be made to work by Hull [5], Fairfull and Hull [6] and Russell *et al.* [7] for examples of work in this area. There is also a growing interest in the properties of cellular materials, for example polymeric foam and natural materials such as wood. This subject has recently been reviewed by Reid *et al.* [8] and analogies between the behaviour of such materials and assemblies of metal tubes have been identified and discussed.

Thin-walled circular tubes ($D/t > 20$, where D is the mean diameter of the tube cross-section and t its wall thickness) compressed axially provide a number of particularly efficient energy-absorbing mechanisms and these are discussed in this paper. They include axial buckling, inversion and axial splitting, the last two usually requiring the use of a profiled die onto which the tube is compressed. The first two modes of deformation have received considerable attention in the literature and formulae have been produced which enable the mean operating loads and energy absorption capacities to be estimated. Notwithstanding this work, rigorous and complete theoretical analyses of the gross deformation fields involved have yet to be produced. The splitting mode was seen as a failure mode for tube inversion [9], but has been developed as an energy absorbing mechanism in its own right.

The results of experiments will be cited in which each of these three primary axial deformation modes have been produced using the same tube stock, so providing a direct comparison between them. Herein, attention is concentrated upon the quasi-static, gross plastic deformation of the various components, although comments are made concerning the important effects arising when the loading is dynamic.

Finally, a brief account is given of the axial buckling of thin-walled square section tubes filled with polyurethane foam. The latter can be modelled as an elastic–plastic–locking material and the interaction between its deformation characteristics and the buckling of the tube results in a particularly efficient energy absorber.

2. EXPERIMENTS AND RESULTS

Seamless mild steel tubes, of 50.8 mm outside diameter and 1.6 mm wall thickness, were used in the experiments conducted using an Instron 1185 universal testing machine at a cross-head speed of 0.167 mm s^{-1}. All the specimens were of 100 mm length. The buckling mode was produced by compressing a tube specimen axially between two flat plates. The inversion and splitting modes were produced by compressing nominally identical specimens onto lubricated dies. The different modes were generated by using hardened dies of different fillet radii. The plane-strain flow stress, σ_0, was measured by performing a lateral (diametral) compression test [10] on a tube of 100 mm length. This provided a value of 732 N mm^{-2} for σ_0.

2.1. *Axial buckling*

Figure 1 shows the load–compression characteristic of the test, and the specimen is also shown in the inset. The axisymmetric (concertina) mode of buckling occurred. A mean load of 80 kN was obtained, with a load fluctuation having peak-to-peak amplitude of 45 kN. The maximum compression possible was 70 mm after which the specimen produced a resistance in excess of 500 kN.

2.2. *External inversion*

Figure 2a shows the load–compression curves from the inversion tests. With dies of radii 4 and 6 mm, inversion was accomplished successfully with mean loads of 85 and 80 kN, respectively. After an initial transient phase during which the leading edge rotates through 270°, the inversion load achieved an essentially constant value. With a 10 mm radius die, the tube flared and cracked. With a 3.2 mm radius die, the tube inverted but the leading edge of the tube pressed against the tube. The consequent increase in resistance to deformation resulted in this tube buckling. Figure 2b shows the deformed specimens for the dies of fillet radius 10, 6 and 4 mm.

2.3. *Axial splitting*

A tube identical to the one which cracked in the inversion test was compressed onto the 10 mm radius die. The tube flared and cracked at five locations around the circumference. The cracks did not appear simultaneously. However, only two cracks propagated and three stopped within 5 mm. It is interesting to note, however, that the two propagating cracks bifurcated successively to produce a total of five cracks. The cracks realigned and were propagating axially again at a compression of approximately 60 mm. Other splitting specimens each had four saw cuts of 3 mm depth introduced symmetrically around their circumference. Cracks started from the tips of these stress raisers and the strips so formed curled up as the tubes were compressed on to the dies. The strips were also flattened in the circumferential direction in the bending process. More details of the splitting mechanism can be found in Ref. [11]. In terms of performance as an energy absorber, an improved arrangement has been devised. These involve the use of a "curl-stopper" plate at a certain stand-off distance, s, from the surface of the die. This plate prevents the strips from curling and forces them to move radially as the compression progresses. Figure 3 shows typical load–deflection curves and deformed specimens for the chosen tubes.

2.4. *Comparison of mechanisms* vis à vis *energy absorbing capacity*

A summary of the principal features of the test results is given in Table 1. The mean load calculations are accurate to 5%. The similarities and differences in the energy absorbing mechanisms will be discussed below but their global effects are evident in the data presented in Table 1. The two modes which do not involve fracture possess a high mean load reflecting the efficient mechanisms consisting principally of circumferential stretching and axial bending about circumferential hinges. The stroke or effective crushing length is of the order of 70% of the tube length. For the splitting mechanism, the lower mean loads are offset by the increased stroke of 95%, resulting in comparable energy absorbing capacities for the smaller die radii. Particular benefits (e.g. an essentially constant steady-state force) accrue from the use of the curl-stopper plate which actually provides a device with comparable if

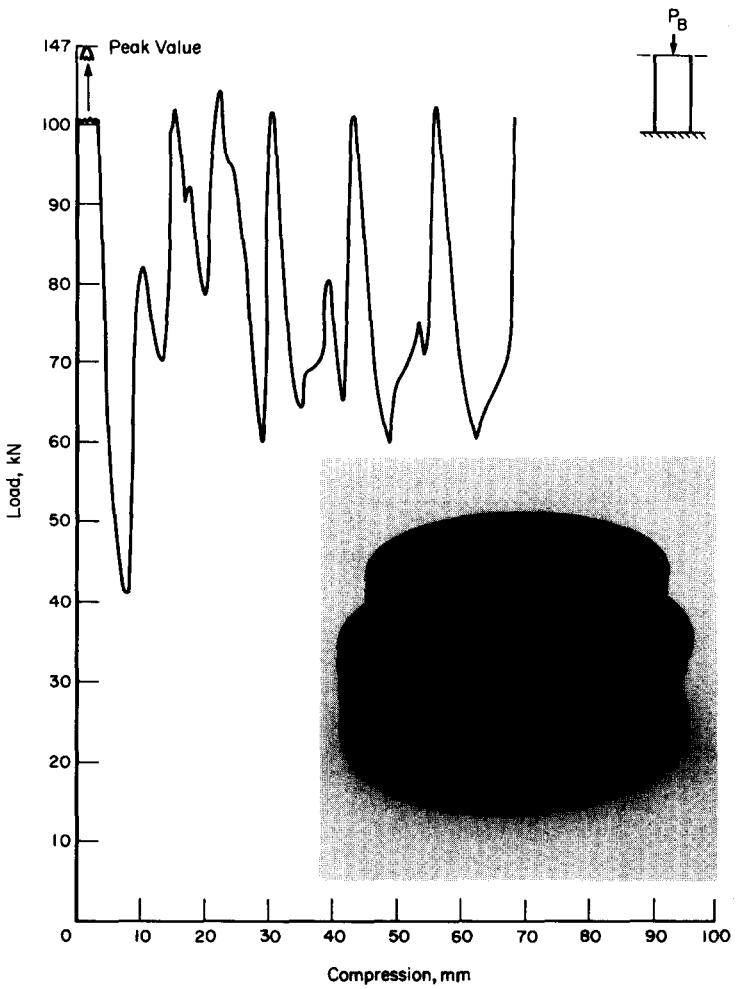

FIG. 1. Load–deflection curve for axial buckling test. Inset shows deformed specimen.

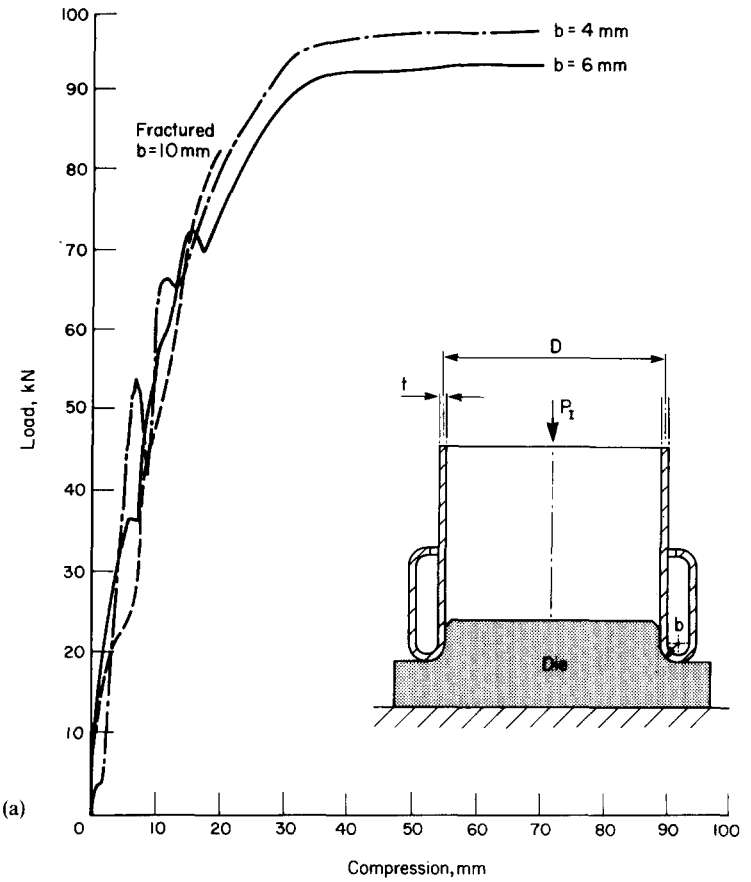

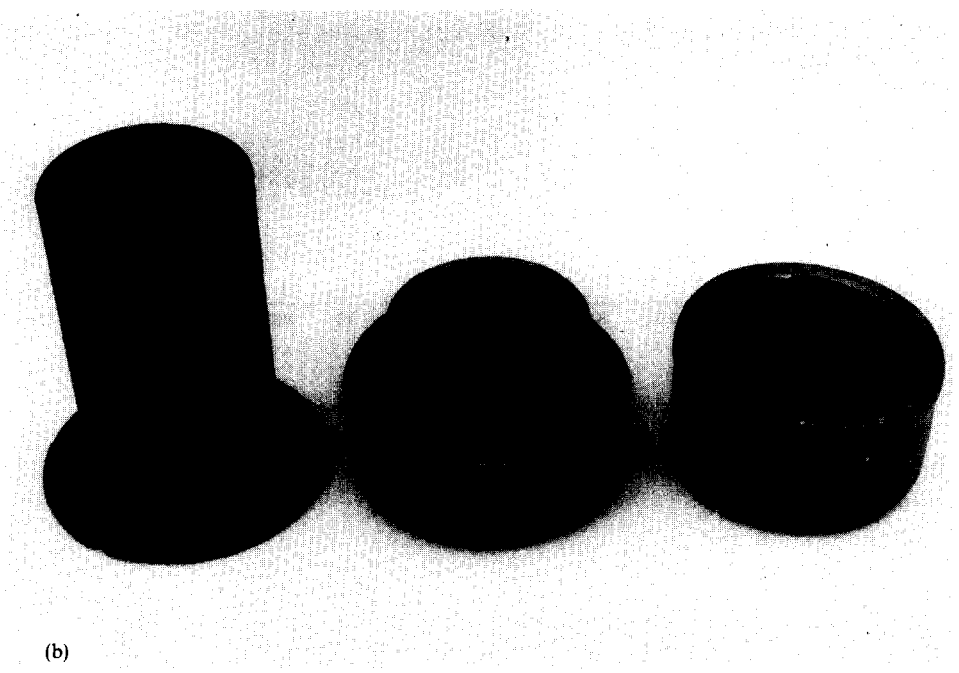

FIG. 2. (a) Load–deflection curve for external inversion tests. (b) Deformed inversion specimens for b = 10, 6 and 4 mm (left to right).

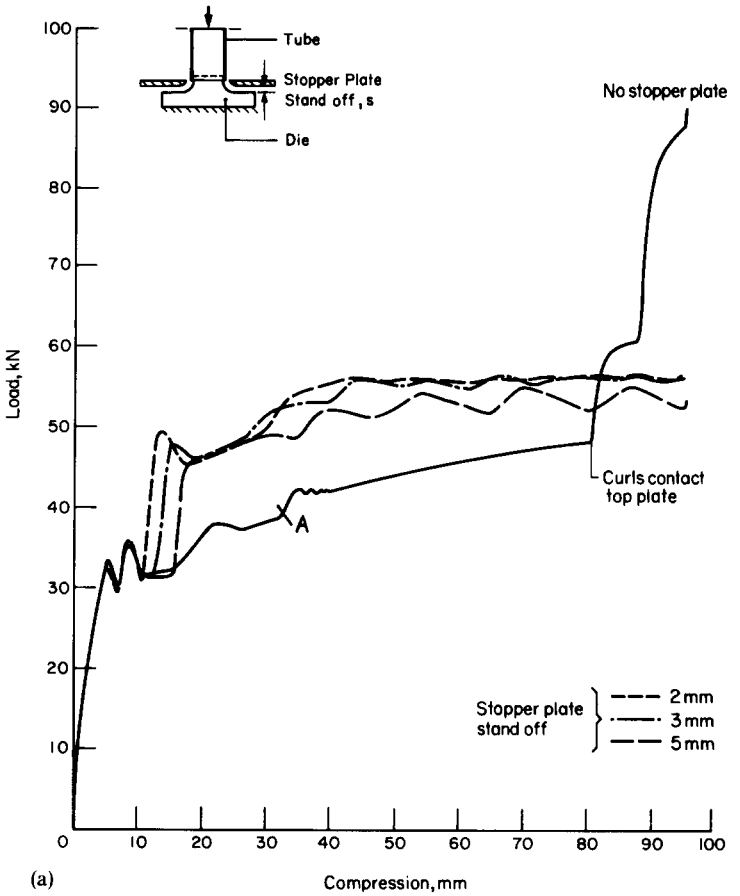

(a)

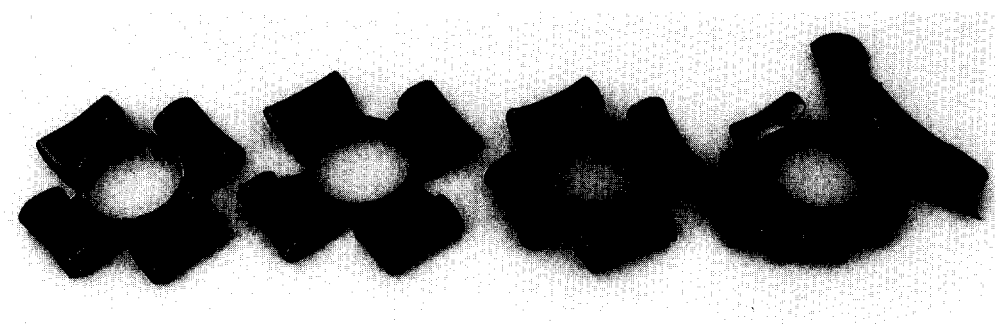

(bi)

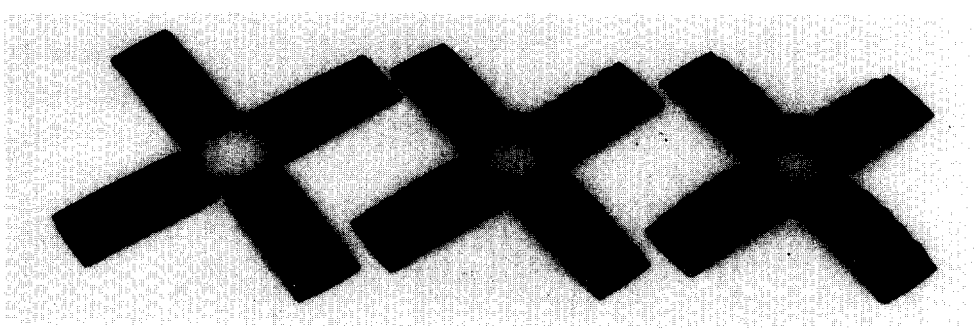

(bii)

FIG. 3. (a) Load–deflection curves for splitting tubes with and without stopper plate. (b) Axial splitting specimens: (i) free to curl. Left to right $b = 10$, 6, 4 mm, $b = 10$ mm, no initial cuts; (ii) curl-stopper tests, $b = 6$ mm. Left to right, $s = 2$, 3, 5 mm.

TABLE 1. SUMMARY OF THE AXIAL TUBE COMPRESSION TESTS

Specimen number	Deformation mode	Mean load (kN)	Compression (= stroke %)	Energy absorbed (J mm^{-1})
1	Axial buckling	80.0	70	56.0
2	Inversion $b = 4$ mm	85.0	66	56.1
3	Inversion $b = 6$ mm	80.0	70	56.0
4	Splitting:curls form $b = 4$ mm	60.0	95	57.0
5	Splitting:curls form $b = 6$ mm	42.5	95	40.4
6	Splitting:curls form $b = 10$ mm	30.0	95	28.5
7	Splitting:curls prevented $s = 5$ mm	50.0	95	47.5
8	Splitting:curls prevented $s = 3$ mm	52.0	95	49.4
9	Splitting:curls prevented $s = 3$ mm	52.5	95	49.9

not better performance than the other two mechanisms and allows for a degree of tuning in the performance of the component.

3. DISCUSSION OF DEFORMATION MECHANISMS AND COMPARISON WITH THEORETICAL MODELS

Both axisymmetric buckling and external inversion involve a combination of meridional (axial) bending and circumferential stretching. Additionally, for inversion using a die, one should make some allowance for the effects of friction. Much has already appeared in the literature on these two mechanisms and so, in the main, attention will be drawn to areas which would benefit from further study.

3.1. *Axisymmetric buckling*

Abramowicz and Jones [12] have provided a comprehensive review and substantial data concerning both axisymmetric and nonaxisymmetric buckling modes. They reworked the rigid–plastic analysis due to Alexander [13], the essence of which is contained in Fig. 4a. The buckling process is assumed to take place in a section of length $2H$ and to consist of a set of three stationary (relative to the material) plastic hinges separating two outward moving portions which undergo circumferential stretching. Common to much of the current work in the analysis of crushing structures, this kinematic field is used to calculate the mean crushing force, P_B, in terms of H. The relevant value of H and, consequently, the value of P_B are determined in terms of the material properties and geometry (R and t) of the tube by minimization, invoking a global minimum work hypothesis, to give [12]:

$$\frac{P_B}{\sigma_0 t^2/4} = 20.79\left(\frac{D}{t}\right)^{1/2} + 11.90 \tag{1}$$

and:

$$\frac{H}{R} = 1.76\left(\frac{t}{D}\right)^{1/2}. \tag{2}$$

For the experiment described above, Eqns (1) and (2) give $P_B = 59.6$ kN and $H = 7.8$ mm. Experimentally, $H = 7.4$ mm approximately, but $P_B = 80$ kN.

This significant underestimate is fairly typical of the predictions of Eqn (1) and was ascribed by Abramowicz and Jones to the assumption that the convolutions flatten into discs. Primarily because of the effects of strain hardening, the convolutions remain, and an approximate analysis [12] gives an effective crush length per convolution, δ_e, given by:

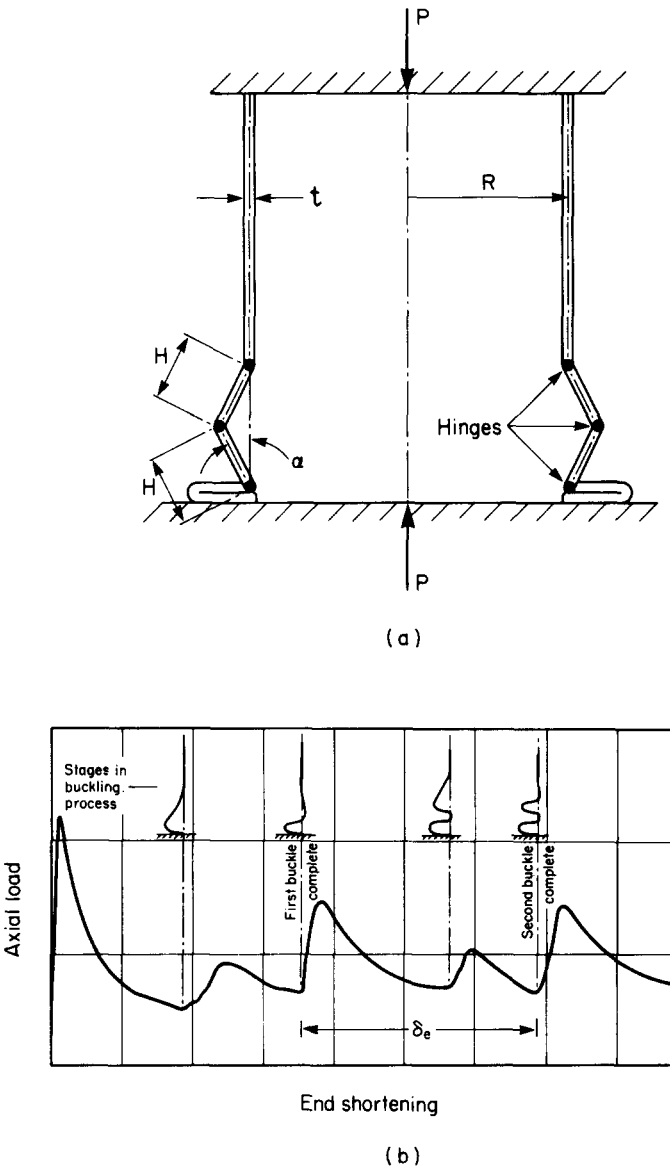

FIG. 4. (a) Axisymmetric axial buckling collapse mechanism due to Alexander [13]. (b) Relationship between generator shape and shape of load–deflection curve for axially symmetric buckling mode (adapted from Ref. [16]).

$$\frac{\delta_e}{2H} = 0.86 - 0.568\left(\frac{t}{D}\right)^{1/2}, \tag{3}$$

Using this reduced crush length instead of $2H$, as assumed in the Alexander analysis, produces a value for P_B of 78.6 kN, which is much closer to the experimental value.

Equation (3) results from an analysis of the geometry of the plastic "hinge" region involving the effects of strain hardening. The analysis, taken from an earlier paper by Abramowicz [14], demonstrates the significant effect that strain hardening can have on the geometry of a structure undergoing gross plastic bending deformation. Similar effects have been analysed in other problems involving regions of intense plastic bending by Reid and Reddy [15]. The important point to note is that the effects of strain hardening show themselves not only in enhanced values for the yield stress (a feature normally accounted for by the use of a flow stress or by estimating a mean strain level appropriate to the process),

but also in local geometry changes which can have significant effects on the loads involved and the way in which the load varies during progressive deformation.

The theory presented by Abramowicz and Jones provides a good method for estimating the mean crushing load and the stroke of an axially buckling tube even in the nonaxisymmetric range. However, a complete theory for predicting the shape of the load–deflection curve is still wanting. The theory as presented gives no estimate for the amplitude of the oscillation of the load about the mean level, let alone the shape of a typical cycle of load. The variation in load shown in Fig. 1 shows a double wave structure within each portion of stroke δ_e.

Figure 4b, adapted from the interesting article by Allan [16], gives an impression of the variation with stroke of the shape of the generator of an axisymmetric buckling tube. These observations are consistent with those made in the test reported above. The waves are laid down in a manner which clearly does not have the symmetry or the simplicity of the model suggested by Alexander. Slight inward, as well as the dominant outward movement of the shell is noticeable, as indeed it was in the tube tested. Several factors suggest that an exploration of the analogous beam–foundation problem may provide a useful step towards understanding this complex problem. In this context the paper by Reid [17] may prove useful, although it is clear that any successful theory would require both large beam deflections and strain hardening to be included in the formulation. The important effects of strain hardening have been demonstrated experimentally by Reddy and Zhang [18] in an interesting paper that highlights the complexities involved in trying to develop theoretical (as opposed to numerical) models for the progressive plastic buckling of tubes.

3.2. *External tube inversion*

Several authors have analysed both external (as depicted in Fig. 2a) [9, 19–24] and internal inversion [9, 19, 25] of metal tubes. An estimate of the steady-state inversion load can be made using the principle of virtual work assuming a deformation field, Fig. 5, in which the tube wall undergoes axial (meridional) bending at A, the point of contact with the die, circumferential stretching in the toroidal region and unbending at B.

Allowance can be made for the effect of friction by estimating the contact pressure, using Coulomb friction and treating the tube–die interface as a tangential velocity discontinuity. The applied force P can be estimated by equating its rate of working with the sum of the rates of energy dissipation in the three principal mechanisms, bending, stretching and interface friction. It is assumed that the material is rigid–perfectly plastic, that there is no interaction between membrane force resultants and bending moments, that the contribution from circumferential bending is negligible, and that the interface pressure is given simply by $p = N_0/r_2$ where $N_0 = \sigma_0 t$ is the membrane yield force per unit length [23]. These calculations lead to:

$$P = 2\pi R\sigma_0 t\left[\ln\left(\frac{a_0}{R}\right) + \frac{t}{4b} + \mu b\int_0^{\phi_0}\frac{\cos\phi}{a}\,\mathrm{d}\phi\right], \tag{4}$$

for $0 < \phi < \pi/2$. For $\pi/2 < \phi_0 < \pi$, the upper limit of the integral is set at $\pi/2$. For $\phi_0 > \pi$, the tube has passed hinge B and Eqn (4) is replaced by the steady-state equation:

$$P_1 = 2\pi R\sigma_0 t\left[\ln\left(1 + \frac{2b}{R}\right) + \frac{t}{2b} + \frac{\mu b}{a}\right]. \tag{5}$$

As shown in Fig. 5, these equations provide a reasonable representation for the transient and steady-state load with $\mu = 0.2$. Also included in Fig. 5 is the initial elastic response derived using the classical ring-edge load solution for a circular cylinder [26].

The dip in the experimental curve and the change in slope at a load of approximately 70 kN correspond to the formation of the lip visible at the leading edge of the inverted tube, the reduction in load in the experiment being associated with circumferential unloading. In this region, Eqns (4) and (5) simply show a change in slope as circumferential stretching gives way to bending at B.

The above analysis assumes rigid–perfectly plastic material behaviour. Recently Reddy [24] has, in an approximate manner, included strain hardening in the analysis of free (i.e.

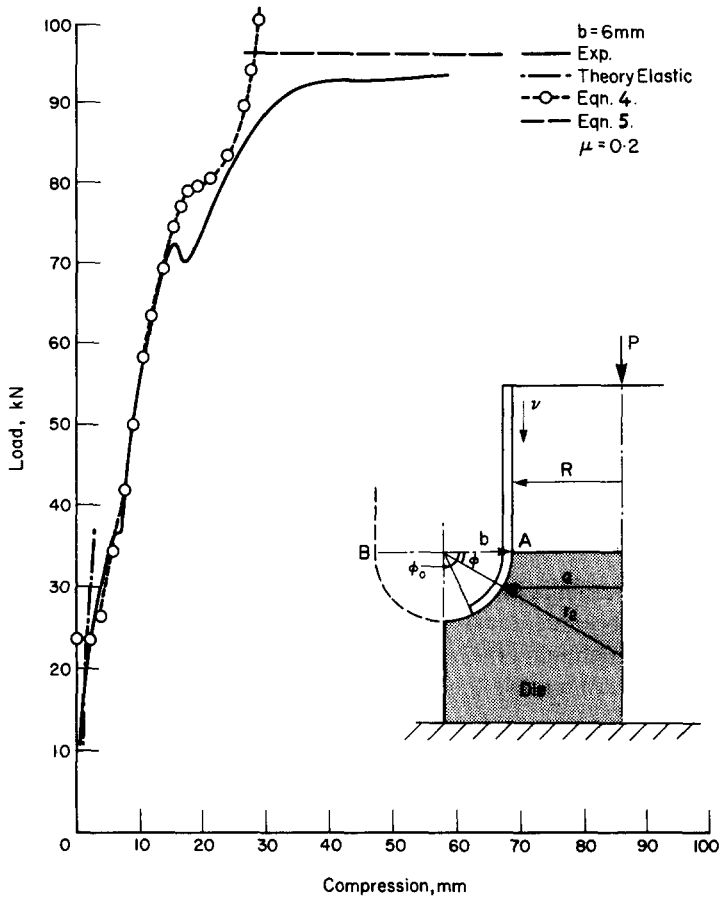

FIG. 5. Comparison between theory and experiment for external tube inversion.

without a die) inversion and has shown that it is responsible for an anomaly in the prediction of the radius of the inverting region highlighted by Calladine [27].

Reddy [19] has also adapted the rigid–perfectly plastic analysis above to treat internal inversion which results in higher loads owing to the thickening of the tube wall. Recently a detailed experimental and finite element analysis of internal inversion of tubes has been completed by Reid *et al.* [25]. An example of the results of this study is shown in Fig. 6. The excellent, detailed agreement between the experimental load–deflection curve and the predictions of the ABAQUS code is the result of removing the kinematic assumptions regarding the conformity of the tube with the die and allowing the contact to develop naturally, as well as being able to include strain hardening and allowing the effects of unloading to show themselves.

3.3. *Axial splitting*

Reddy and Reid [11] have provided a description of circular tubes (with and without initial slots cut into the leading edge) being split by compression onto dies of various radii. The results shown in Fig. 3 convey the qualitative features of these tests including the effect of using a curl-stopper plate. The latter is a particularly useful modification to the basic splitting and curling mechanism, since it removes the hardening characteristic of the load–deflection curve. This results from the increased frictional contributions and additional plastic deformation which occurs when the curls are forced to reduce in radius as they coil following point A in Fig. 3.

If no slots are cut into the leading edge of the tubes, the experimental evidence [11] is that a characteristic number of fractures is produced in the steady state. The five fractures produced in the specimen compressed onto the 10 mm radius die provide a typical

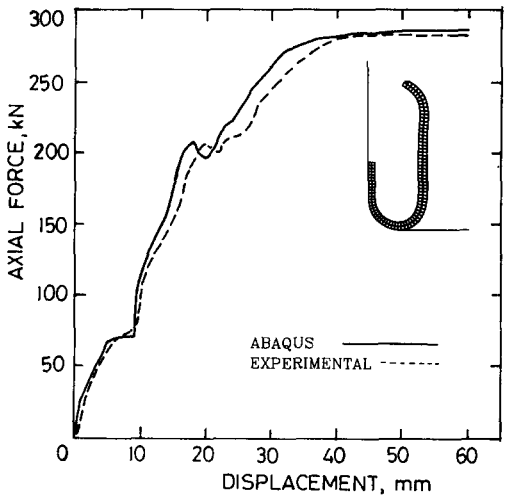

Tube: O.D. = 101.6mm t = 2.0mm
leading edge chamfer radius = 1mm

Die: radius = 10mm, clearance = 0.25mm

Material properties:

Steel tube: $E = 200GN/m^2$ $\sigma_0 = 570MN/m^2$

$E_p = 264MN/m^2$

Friction: $\mu = 0.15$

FIG. 6. Comparison between computed (ABAQUS) and experimental load–deflection curves for an inwardly inverted metal tube.

example of this, the steady state being achieved following a crack initiation stage and a series of bifurcations. The linking of the number of fractures to the material properties requires explanation, but it is relatively unimportant from the point of view of energy absorption and indeed it would be preferable to remove the load fluctuations associated with this transient phase by pre-triggering a certain number of cracks. One practically important feature of the characteristic number of cracks for a given tube is that it provides an upper limit on the number of fractures that can be maintained in the tube. Attempts to exceed this number usually result in a number of the cracks not propagating. A simple minimum energy argument has established that an estimate can be made of the number of fractures initiated [28].

Since five cracks were produced in an untriggered tube, four slots were cut into the remaining specimens. This creates a situation similar to that examined by Stronge *et al.* [29] who performed splitting and curling tests on square tubes of aluminium and mild steel, the deformation being achieved using contoured dies. In earlier work (referred to in Ref. [29]) the mechanisms had been achieved by compressing tubes with sawcuts at each corner on to a flat plate. Stronge *et al.* [29] developed a rate equation for the latter situation which contained contributions to the energy dissipation rate from plastic bending, fracture and friction. In this, the contact force between the tube walls and the plane was relatively easy to define and locate. An interesting discussion was provided of the role of strain hardening in the deformation of the curled plates, although these effects were ignored in deducing quantitative information from the model.

It has been noted that in the tests performed, meridional bending, circumferential flattening and crack propagation occurred. Incorporating these into a rate equation for

splitting and curling leads to [23]:

$$P_s = \frac{2\pi R\sigma_0 t\left[\frac{t}{4b} + \frac{t}{4R}\right] + nG_c t}{1 - \mu/\sin\alpha(1+\mu^2)^{1/2}}, \tag{6}$$

where b is the die radius as before, n is the number of fractures and G_c is the fracture toughness (approximately 100 kJ m^{-2} for mild steel) of the material. α is the inclination of the resultant force on each strip to the horizontal.

The case assumed by Stronge *et al.* [29] corresponds to $\alpha = \pi/2 + \phi$ where $\tan\phi = \mu$ and the denominator reduces to $1 - \mu$. The estimate is clearly sensitive to both μ and α. In Ref. [11] it is suggested that $\alpha = \pi/4$ is a reasonable first estimate representing the direction of the resultant force. For a different batch of mild steel tubes ($\sigma_0 = 800$ N mm^{-2}), splitting into twelve strips, $\mu = 0.2$ provided a good estimate for P_s. In the present tests, Fig. 7 shows that a higher value of approximately 0.45 is required to match the experimental data. This probably reflects the more severe loading conditions at the edges of the four strips compared with the case when twelve strips are produced. As with the inversion problem, in order to incorporate more adequately the effects of friction, a more accurate modelling procedure (such as finite element analysis) is required to remove the *a priori* assumptions about the nature of the contact between the tube and the die.

The curl prevention tests involve both extra bending plastic work [$t/4b$ is replaced by $t/2b$ in Eqn (6)] as the strips are unbent and, more problematical, extra frictional dissipation. The latter presumably leads to a modification of the die contact force distribution which requires further study. The addition of the extra bending term into Eqn (6) results in an estimate of 60 kN for the three curl-prevention tests. It is worth noting that consideration of the bending moment distribution in the curls, as outlined in Ref. [29], leads to the conclusion that strain hardening again plays an important role in controlling the deformation field in the bending regions. This too would no doubt be clarified in a more detailed and accurate numerical model.

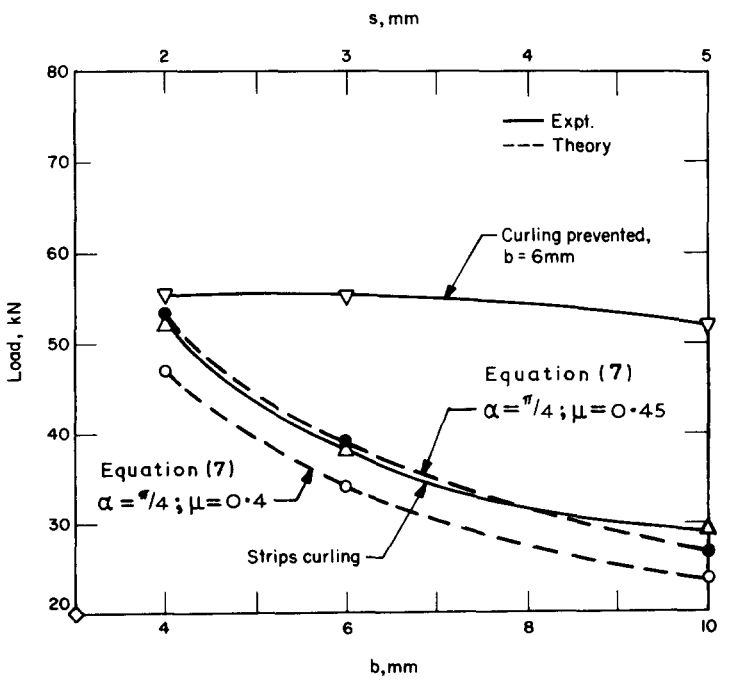

FIG. 7. Operating loads for tube splitting and curling compared with predictions of Eqn (6) and operating loads for curl-stopper tests using a 6 mm die radius.

3.4. *Effects of loading rate*

The initial yield stress of mild steel increases significantly with strain rate and this is reflected in the operating loads of energy absorbing devices whose behaviour is dominated by plastic deformation [1]. The mean load, P_B, for axial buckling increases under dynamic loading conditions. Abramowicz and Jones [12] suggest a dynamic enhancement factor, m, given by:

$$m = 1 + \left\{ \frac{0.25V}{6844R[0.86 - 0.568(t/D)^{1/2}} \right\}^{1/3.91}, \tag{7}$$

for axisymmetric axial buckling, where V is the impact speed. This makes allowance for the fact that the strain-rate enhancement reduces for large strains. A similar factor applied to the inversion tube data produces results consistent with the experimental data, although P_I can decrease for some materials due to changes in frictional conditions under dynamic loading.

Stronge *et al.* [29] estimated a factor of 2.5–3 for a dynamic splitting of mild steel square tubes. This was partly ascribed to strain-rate enhancement of the yield stress and partly to increases in the value of μ. The results of Reddy and Reid [11] indicate that where a larger number of fractures are produced (say 8–12), the operating force may not differ significantly from the quasi-static value. It should be noted that in the work described in Ref. [11], dynamic forces were measured directly, whereas in Ref. [29] they were estimated from energy considerations. The result in Ref. [11] may not be too surprising, since the increase in flow stress resulting from increasing the strain rate is often accompanied by a reduction in the strain to fracture which would be reflected by lower dynamic G_c values. Thornton and Dharan [30] report that the flow stress of an aluminium–magnesium alloy foam reduces under high-rate loading. They state that "notch sensitivity increases with increase in strain rate, and so the strength of the foam would be decreased." Where fracture is a significant mechanism in the deformation field, caution should be exercised in predicting the influence of increased strain rate.

The second effect of increased loading rate is the introduction of inertia forces which can influence the mode of deformation of the component. Broadly speaking, most impact energy absorbing components deform in the same mode as that produced under static loading. The term quasi-static response is often reserved for this kind of behaviour. Consequently, the forces involved can be calculated on the basis of static plastic collapse methods as indicated above. Dynamic effects are then accounted for by using an enhancement factor such as that given in Eqn (7). However, this only accounts for the strain-rate sensitivity of the yield stress of the material.

Inertia effects are obviously present whenever impact loading occurs, and they become important when they introduce a delay in the initiation of the quasi-static mode of deformation (sometimes referred to as the modal response). Often this pre-modal phase occupies a very short time compared with the duration of the deformation and its effects can be neglected. This is especially so when the ratio of the mass of the body decelerated by the energy absorbing component to the mass of the component is large, say greater than 10. If this is not so, then a complete understanding of the performance of the energy absorber can only be achieved by modelling both the pre-modal and modal phase.

It would appear that these effects are most noticeable in so-called Type II structures [31–33] which have an unstable (reducing) static force–deflection characteristic. Relatively few detailed analyses of energy absorbers have been performed to investigate this point. A more detailed discussion of the matter is provided by Reid *et al.* [8] in the context of cellular structures and cellular materials where inertia-dominated behaviour for wood has been clearly identified. The fact that the three modes of deformation for circular tubes described above each involve axial loads and the load–deflection characteristics in each case have instabilities associated with them, especially in the initial stages of deformation, suggests that inertia effects should be carefully considered for these components. The work in Ref. [25] is part of such a study for internal tube inversion. These comments draw attention to the need for reasonably accurate predictions of load–deflection characteristics so that the source of any instabilities can be identified. Our recent work on internal

inversion has shown that the inertia effects associated with these instabilities can give rise to forces which are in excess of the steady state (dynamic) operating forces. Thus, from a design point of view, their assessment is of some importance.

4. AXIAL CRUSHING OF FILLED THIN-WALLED SQUARE SECTION TUBES

An interesting example of the combined use of different materials in an energy absorbing component is to be found in the use of polyurethane foam (an elastic–plastic–locking material, see Ref. [8]) to stabilize and improve the performance of thin-walled tubes. Typically the side-length to thickness ratio is approximately 100 in these tubes. This aspect ratio is not untypical of that found in automobile structures. A few examples will be cited here to convey the nature of the interaction. More details on the behaviour of sheet metal tubes subjected to axial crushing can be found in Refs [34–37] whilst details of fibre-reinforced tubes which lie outside the scope of the present paper are given in Ref. [7].

4.1. *Effect of foam filling on crushing mechanism*

Axially compressed thick-walled square section metal tubes exhibit folding mechanisms similar to that shown in Fig. 1 for a circular tube. Progressive buckling occurs from one end of the specimen, the folds being contiguous. Such modes are described as *compact*. This contrasts with the *noncompact* modes produced in thinner tubes in which the fold mechanisms are separated by a distance approximately equal to the side length of the square tube. These two modes are shown in Fig. 8. Similar behaviour is observed in tubes of rectangular cross-section [34].

Not only does noncompact behaviour lead to lower specific energy absorption capacities, but it can also lead to global instability due to the formation of Euler-type failure mechanisms. The use of polyurethane foam as a filler material to stabilize the behaviour of structures used for energy absorption was first explored by Lampinen and Jeryan [38]. They concluded that it is more effective to increase the thickness of the metal sheet than to fill the sections they examined with the foam. However, the studies described in Refs [34] and [35] show that noncompact behaviour can be transformed to compact behaviour by foam filling; this is demonstrated in Fig. 9, and herein lies a major advantage.

4.2. *Mean crushing force prediction for filled tubes*

The walls of the tube buckle under axial load and the transverse displacement of the walls imposes loads on the foam core. Treating each panel of the tube as a plate on a foam foundation allows estimates to be made of the mean crushing strength of the tube [34]. Noncompact behaviour stems from the fact that, because the tubes are thin-walled, they deform in an elastic buckling mode, the half-wavelength of which is equal to the side length of the tube. The analysis of an elastic plate resting on an elastic foundation shows that the half-wavelength of the elastic buckling pattern, λ_e, reduces with increasing foam density ρ_f [34]. When λ_e becomes close to the extent of the plastic fold mechanism of the tube, λ_p, the deformation mode becomes compact rather than noncompact. The theoretical model that provides the mean plastic crushing loads [34] is based upon the analysis of the folding mechanism in square tubes provided by Wierzbicki and Abramowicz [39]. The simple argument used is that the onset of locking in the foam arrests the collapse of the folding segment of the tube. The degree of crushing is defined by an angle α_0 where:

$$\alpha_0 = \cos^{-1}[1 - \varepsilon_l] \tag{8}$$

and ε_l is the locking strain of the foam.

For a square tube of side length c and wall thickness t made from a material with yield stress σ_0 and filled with foam of crush strength σ_f and locking strain ε_l, it is shown in Ref. [34] that its mean crushing load is:

$$P_{mf} = 3\sigma_0 \sqrt[3]{g_1 g_2 g_3 c t^5} + \sigma_f c^2 . \tag{9}$$

where g_1, g_2 and g_3 are known functions of α_0. Simple strain-rate enhancement factors can be calculated to convert Eqn (8) into an appropriate form for dynamic crushing which agrees well with experimental data, as demonstrated in Fig. 10.

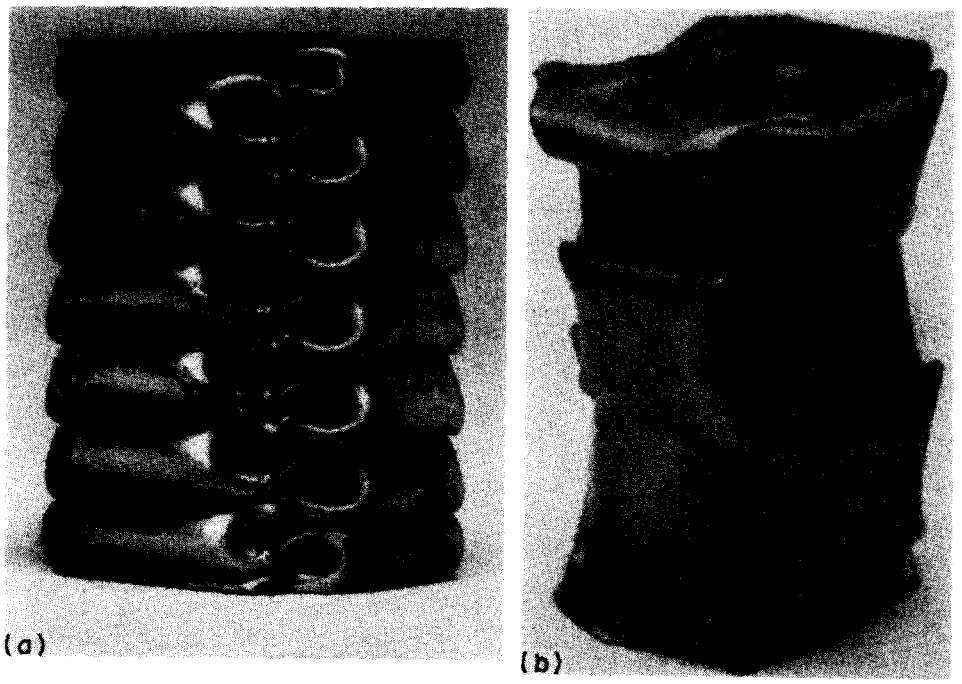

FIG. 8. Axially crushed square tubes: (a) compact crusing mode (aluminium tube $c/t = 32.4$); and (b) noncompact crushing mode (mild steel tube $c/t \approx 100$).

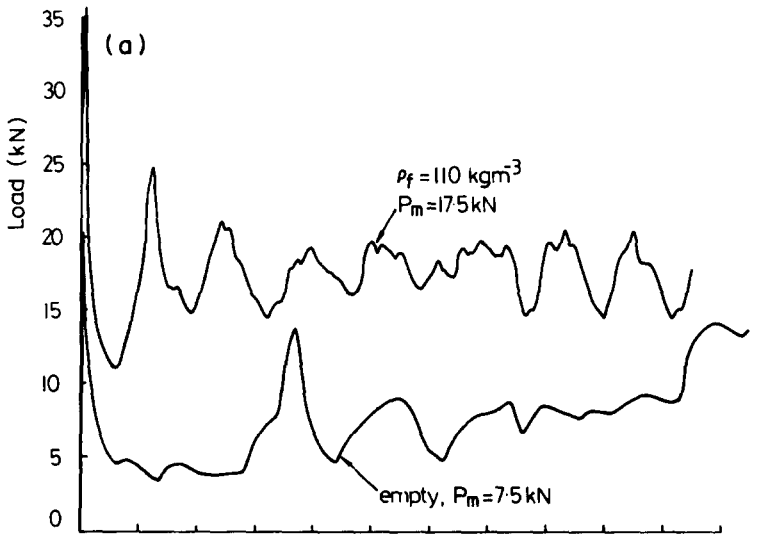

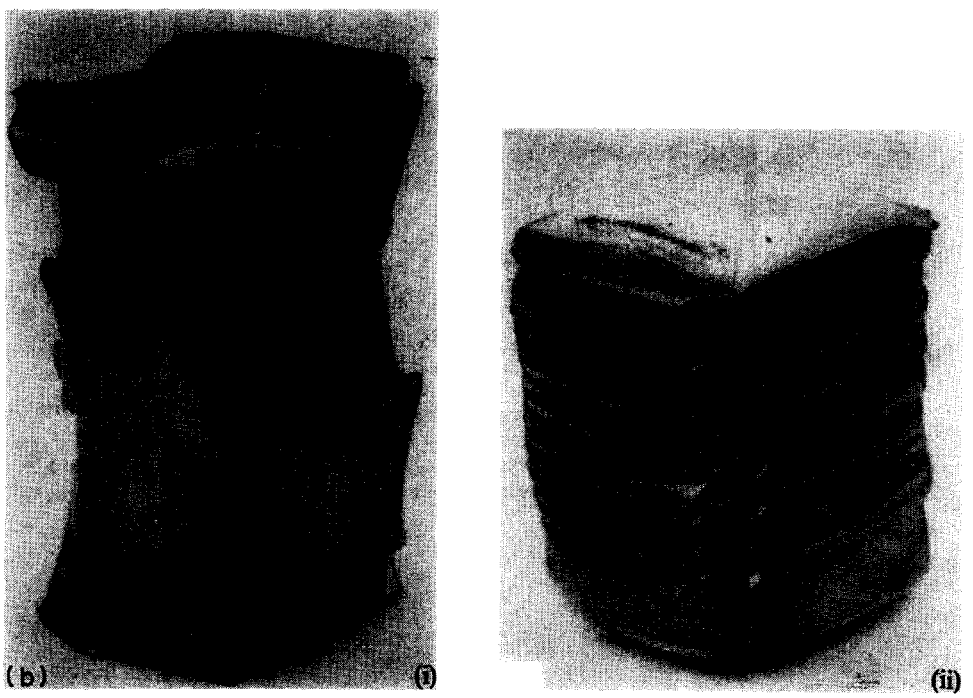

FIG. 9. (a) Load–compression curves for empty and filled square tubes, 75 mm × 75 mm, t = 0.76 mm. (b) Deformed specimens: (i) empty; (ii) filled, ρ_f = 110 kg m^{-3}.

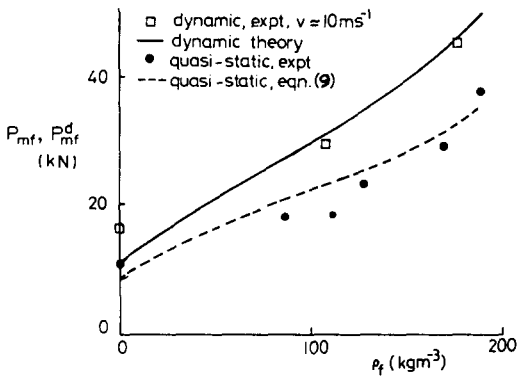

FIG. 10. Variation of experimental and theoretical mean loads with foam density for 75 mm × 75 mm × 0.76 mm square tubes under quasi-static and dynamic ($v_0 \approx 10\ \mathrm{m\,s^{-1}}$) loading.

5. FINAL COMMENTS

Fundamental to the use of many metal components as energy absorbers is the ductility which permits large plastic strains to be generated and large geometry changes to be achieved without global failure. Plastic deformation is therefore a major mechanism by which energy can be dissipated. It has been shown that mechanisms which involve fracture can also find application in this field as exemplified by the splitting of metal tubes. Idealized rigid–plastic analyses based upon assumed kinematic deformation fields have been shown to be successful in estimating the mean operating loads for the tube components described.

However, the need for more accurate and detailed representations of the load–deflection characteristics which reveal the occurrence and extent of instabilities in the deformation process or account reliably for the effects of friction poses formidable problems. Kinematic approaches would seem to be inappropriate and the role of material strain hardening cannot be ignored in many cases. When dynamic effects (including the influence of strain rate on the yield stress and fracture strain and inertia) are present, the modelling becomes even more complex. From a basic design point of view, it is important to have estimates for the operating loads and energy absorbing capacities of components and the existing approaches are sufficient. However, if more accurate predictions of load pulses are required, then more sophisticated theoretical models must be constructed or detailed numerical analyses using finite elements performed.

Examining the crushing performance of thin-walled tubes has shown that significant improvements can be achieved by using composite structures, i.e. structural elements comprised of more than one material. It is clear that by choosing compatible material properties one can generate beneficial interactions between the components. Greater stability and genuine increases in specific energy absorption capacity can both be achieved. Simple rigid–plastic kinematic models into which the locking properties of the foam are included produce useful estimates of the mean crushing forces.

Acknowledgement—The author is grateful to Dr T. Y. Reddy and Mr J. Harrigan for helpful discussions and comments during the preparation of this paper.

REFERENCES

1. W. JOHNSON and S. R. REID, Metallic energy dissipation systems. *Appl. Mech. Update* (edited by C. R. STEELE), pp. 303–319. ASME, New York (1986).
2. N. JONES and T. WIERZBICKI (Eds), *Structural Crashworthiness*. Butterworths, London (1983).
3. T. WIERZBICKI and N. JONES (Eds), *Structural Failure*. Wiley, New York (1989).
4. N. JONES and T. WIERZBICKI (Eds), *Structural Crashworthiness and Failure*. Elsevier Applied Science, Amsterdam (1993).
5. D. HULL, Axial crushing of fibre-reinforced composite tubes, in *Structural Crashworthiness* (edited by N. JONES and T. WIERZBICKI), pp. 118–135. Butterworths, London (1983).
6. A. H. FAIRFULL and D. HULL, Energy absorption of polymer matrix composite structures: frictional effects, in *Structural Failure* (edited by T. WIERZBICKI and N. JONES), pp. 255–279. Wiley, New York (1989).

7. A. T. RUSSELL, T. Y. REDDY, S. R. REID and P. W. SODEN, Quasi-static and dynamic axial crushing of foam-filled FRP tubes, in *Composite Materials Technology* 1991 (edited by D. HUI and T. J. KOZIK, *ASME PD*-Vol. 37, pp. 145–152 (1991).
8. S. R. REID, T. Y. REDDY and C. PENG, Dynamic compression of cellular structures and materials, in *Structural Crashworthiness and Failure* (edited by N. JONES and T. WIERZBICKI). Wiley, New York (1989).
9. S. T. S. AL-HASSANI, W. JOHNSON, and W. T. LOWE, Characteristics of inversion tubes under axial loading. *J. Mech. Engng Sci.* **14**, 370–381 (1972).
10. T. Y. REDDY and S. R. REID, On obtaining material properties from the ring compression test. *Nucl. Engng Design* **52**, 257–263 (1979).
11. T. Y. REDDY and S. R. REID, Axial splitting of circular metal tubes. *Int. J. Mech. Sci.* **28**, 111–131 (1986).
12. W. ABRAMOWICZ and N. JONES, Dynamic axial crushing of circular tubes. *Int. J. Impact Engng* **2**, 263–281 (1984).
13. J. M. ALEXANDER, An approximate analysis of the collapse of thin cylindrical shells under axial loading. *Quart. J. Mech. Appl. Math.* **13**, 10–15 (1960).
14. W. ABRAMOWICZ, The effective crushing distance in axially compressed thin-walled metal columns. *Int. J. Impact Engng* **1**, 309–317 (1983).
15. S. R. REID and T. Y. REDDY, Effects of strain hardening on the lateral compression of tubes between rigid plates. *Int. J. Solids Struct.* **14**, 213–225 (1978).
16. T. ALLAN, Investigation of the behaviour of cylindrical tubes subject to axial compressive forces. *J. Mech. Engng Sci.* **10**, 182–197 (1968).
17. S. R. REID, Influence of geometrical parameters on the mode of collapse of a "pinched" rigid–plastic cylindrical shell. *Int. J. Solids Struct.* **14**, 1027–1043 (1978).
18. T. Y. REDDY and E. ZHANG, The effect of strain-hardening on the behaviour of axially crushed cylindrical tubes, in *Advances in Engineering Plasticity and its Applications* (edited by W. B. LEE), pp. 755–762. Elsevier, Amsterdam (1993).
19. T. Y. REDDY, Tube inversion—an experiment in plasticity. *Int. J. Mech. Engng Educ.* **17**, 277–292 (1989).
20. L. R. GUIST and D. P. MARBLE, Prediction of the inversion load of a circular tube. NASA Technical Note TN D-3622 (1966).
21. H. A. AL-QURESHI and G. A. DEMORAIS, Analysis of multi-inversion of tube ends. ASME Paper No. 77-DE-35 (1977).
22. A. N. KINKEAD, Analysis for inversion load and energy absorption of a circular tube. *J. Strain Anal.* **18**, 177–188 (1983).
23. S. R. REID and T. Y. REDDY, Axially loaded metal tubes as impact energy absorbers. *Proc. IUTAM Symp. on Inelastic Behaviour of Plates and Shells* (edited by L. BEVILACQUA, R. FEIJOO and R. VALID), pp. 569–595. Springer, Heidelberg (1986).
24. T. Y. REDDY, Guist and Marble revisited—on the natural knuckle radius in tube inversion. *Int. J. Mech. Sci.* **34**, 761–768 (1992).
25. S. R. REID, J. HARRIGAN and P. D. SODEN, Internal tube inversion. *Int. J. Mech. Sci.* (submitted) (1993).
26. S. P. TIMOSHENKO and S. WOINOWSKY-KRIEGER, *Theory of Plates and Shells*, Chap. 15. McGraw-Hill, New York (1959).
27. C. R. CALLADINE, Analysis of large plastic deformations in shell structures, in *Inelastic Behaviour of Plates and Shells* (edited by L. BEVILACQUA, R. FEIJOO and R. VALID), pp. 69–101. Springer, Berlin (1986).
28. A. G. ATKINS, On the number of cracks in the axial splitting of ductile metal tubes. *Int. J. Mech. Sci.* **29**, 115–121 (1987).
29. W. J. STRONGE, T. X. YU and W. JOHNSON, Energy dissipation by splitting and curling of tubes, in *Structural Impact and Crashworthiness* (edited by J. MORTON), Vol. 2, pp. 576–587. Elsevier Applied Science, Amsterdam (1984).
30. P. H. THORNTON and C. K. H. DHARAN, The dynamics of structural collapse. *Mater. Sci. Engng* **18**, 97–120 (1975).
31. C. R. CALLADINE and R. W. ENGLISH, Strain-rate and inertia effects in the collapse of two types of energy-absorbing structure. *Int. J. Mech. Sci.* **26**, 689–701 (1984).
32. T. G. ZHANG and T. X. YU, A note on a velocity sensitive energy absorbing structure. *Int. J. Impact Engng* **8**, 43–51 (1989).
33. L. L. TAN and C. R. CALLADINE, Inertia and strain-rate effects in a simple plate-structure under impact loading. *Int. J. Impact Engng* **11**, 349–377 (1991).
34. S. R. REID, T. Y. REDDY and M. D. GRAY, Static and dynamic axial crushing of foam-filled sheet metal tubes. *Int. J. Mech. Sci.* **28**, 295–322 (1986).
35. S. R. REID and T. Y REDDY, Static and dynamic crushing of tapered sheet metal tubes of rectangular cross-section. *Int. J. Mech. Sci.* **28**, 623–637 (1986).
36. S. R. REID and T. Y. REDDY, Axial crushing of foam-filled tapered sheet metal tubes. *Int. J. Mech. Sci.* **28**, 643–656 (1986).
37. T. Y. REDDY and R. J. WALL, Axial compression of foam-filled thin-walled circular tubes. *Int. J. Impact Engng* **7**, 151–166 (1988).
38. B. E. LAMPINEN and R. A. JERYAN, Effectiveness of polyurethane foam in energy absorbing structures. *Trans. SAE* **91**, 2059–2076 (1982).
39. T. WIERZBICKI and W. ABRAMOWICZ, On the crushing mechanics of thin-walled structures. *J. Appl. Mech.* **50**, 727–734 (1983).